Hall effect and the magnetotransport properties of $Co_2MnSi_{1-x}Al_x$ Heusler alloys

Joseph C. Prestigiacomo, David P. Young, Philip W. Adams, and Shane Stadler[a)]
Department of Physics and Astronomy, Louisiana State University, Baton Rouge, Louisiana 70803, USA

(Received 6 December 2013; accepted 10 January 2014; published online 27 January 2014)

We have investigated the transport properties of the quaternary Heusler alloys $Co_2MnSi_{1-x}Al_x$ ($0 \leq x \leq 1$), which have been theoretically predicted to develop a half-metallic band structure as $x \rightarrow 0$. Resistivity versus temperature measurements as a function of Al concentration (x) revealed a systematic reduction in the residual resistivity ratio as well as a transition from weakly localized to half-metallic conduction as $x \rightarrow 0$. From measurements of the ordinary and anomalous Hall effects, the charge carrier concentration was found to increase, while the anomalous Hall coefficient decreased by nearly an order of magnitude with each sample as $x \rightarrow 0$ ($\Delta x = 0.25$.). Scaling of the anomalous Hall effect with longitudinal resistivity reveals that both the skew-scattering and intrinsic contributions grow quickly as $x \rightarrow 1$, indicating that disorder and band-structure effects cause the large anomalous Hall effect magnitudes observed for Co_2MnAl. © *2014 AIP Publishing LLC*. [http://dx.doi.org/10.1063/1.4862966]

I. INTRODUCTION

The quinternary full-Heusler compound $Co_2(Cr_{1-y}Mn_y)(Si_{1-x}Al_x)$ with the $L2_1$ crystal structure has proved to be a useful system to investigate the optimization of half-metallic behavior through doping.[1] A particularly interesting subset of this class of compounds is obtained with $y = 1$ and a variable Al concentration, $Co_2MnSi_{1-x}Al_x$. Theoretically, it is expected that, as x increases from 0 to 1, the Fermi energy (E_F) will shift within the minority spin band from the center of a relatively wide gap (~0.6 eV) to the upper edge of the valence band. Recently, this shift was observed in the tunneling conductance (G-V) measurements of magnetic tunnel junctions (MTJs) composed of B2-ordered epitaxial films having different Al concentrations (x).[2] Several desirable properties are found in the full-stoichiometric compounds. Co_2MnSi ($x = 0$) is well-known for its potential use in spintronic applications. It has an extremely high Curie temperature of ~1000 K,[3,4] and produces giant tunnel magnetoresistance ratios (TMRs) when used as an electrode in MTJs.[5] The compound Co_2MnAl ($x = 1$) has not been predicted to be fully spin-polarized; however, its high Curie temperature of ~700 K,[3,6] combined with its large anomalous Hall effect (AHE),[7] has redeemed it as a valuable material for Hall effect sensors in automotive applications.[8]

In light of the above mentioned potential applications of the full-stoichiometric compounds, it is worthwhile to investigate the physical properties of $Co_2MnSi_{1-x}Al_x$ as a function of Al content. The dependence of the magnetic and structural properties of $Co_2MnSi_{1-x}Al_x$ on Al content has been previously investigated.[3,9,10] Notably, in Ref. 3, it was shown that the bulk polycrystalline series follows the Slater-Pauling rule, as predicted by the theory of spin-polarization in Heusler alloys.[11] This rule relates the total number of valence electrons in a unit cell to the total saturation magnetization in units of Bohr magnetons per formula unit, meaning that the magnetization can be precisely controlled by tuning the value of x.

Since $Co_2MnSi_{1-x}Al_x$ is predicted to have spin-polarized charge carriers, carrier-dependent magnetotransport measurements should provide insight into interesting electrical conduction properties when the Fermi level is systematically shifted through majority/minority bands by doping. A particularly revealing phenomenon, and therefore an important tool, is the Hall effect, whose ordinary and anomalous contributions contain terms sensitive to the details of the Fermi surface.[12,13] Indeed, it has been theoretically shown that Co_2MnAl may exhibit a fully spin-polarized Hall current despite its only partially spin-polarized band structure.[14] Therefore, this study includes measurements of the magnetoresistance (MR) and the Hall resistivity of bulk polycrystalline $Co_2MnSi_{1-x}Al_x$ ($x = 0$, 0.25, 0.5, 0.75, and 1) as a function of temperature and applied magnetic field. Interestingly, an applied field did not generate a detectable Hall voltage in Co_2MnSi ($x = 0$). Moreover, negligible field response was observed in the MR for all x, other than the small artifacts leaked in by the Hall effect due to slight lead misalignments. The absence of MR in Co_2MnSi is consistent with previous observations in single-crystals[15] and probably indicates negligible spin-disorder scattering.

II. EXPERIMENTAL DETAILS

Bulk $Co_2MnSi_{1-x}Al_x$ ($x = 0$, 0.25, 0.5, 0.75, and 1) samples were synthesized by rf-induction melting in a 4N purity Ar atmosphere. The polycrystalline samples were annealed at 1100 °C for 3 days and then at 600 °C for an additional 5 days. X-ray powder diffraction was used to confirm that the $L2_1$ phase was obtained in all samples and that there were no impurity phases (see Fig. 1). The linear dependence of the lattice constant (a) with Al content (x) was determined from the shift in the $L2_1$ 220 peak. This is in agreement with Vegard's law[16] and suggests that a homogenous distribution of Si/Al was achieved throughout the bulk.

[a)]Author to whom correspondence should be addressed. Electronic mail: stadler@phys.lsu.edu

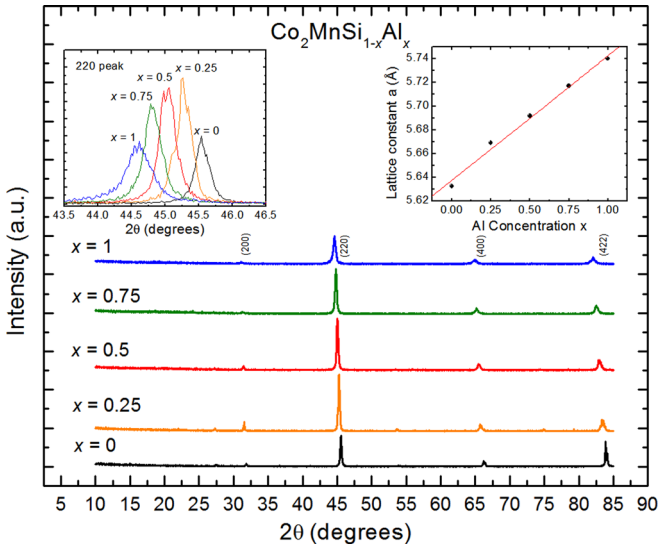

FIG. 1. The X-ray powder diffraction patterns for $Co_2MnSi_{1-x}Al_x$ ($x = 0$, 0.25, 0.5, 0.75, and 1). Left inset: Magnified view of the 220 peak of the powder XRD, used to calculate a. Right inset: The lattice constant (a) versus Al concentration (x). The red line is a guide to the eye showing the close agreement with Vegard's law.

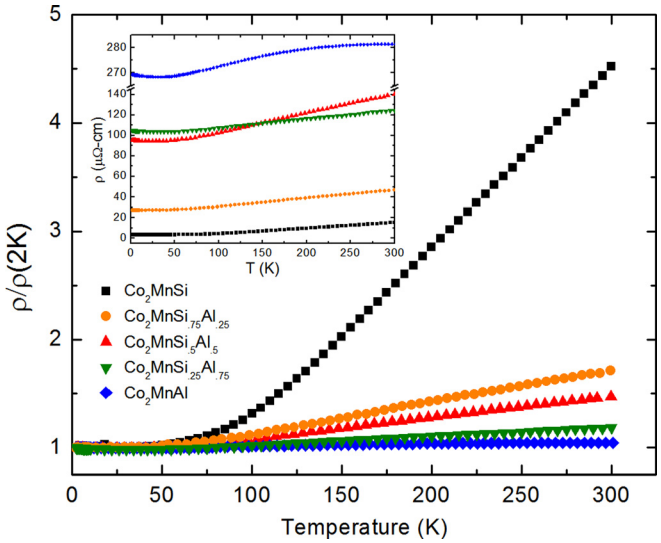

FIG. 2. The resistivity as a function of temperature curves normalized by their values at 2 K. Inset: The absolute resistivity as a function of temperature.

Magnetization data were collected with a Quantum Design Magnetic Properties Measurement System (MPMS) SQUID magnetometer with magnetic fields between $B = \pm 7$ T and in the temperature range $T = 2$ to 400 K. Resistivity measurements were performed at temperatures between 2 and 400 K in applied magnetic fields between ± 9 T using a standard four-wire technique with a QD PPMS equipped with the AC transport option. Sample cuts of approximately $2.5 \times 1.5 \times 0.4$ mm^3 were taken from the interior of the ingots, polished, and then sonicated in acetone for 1 h before attaching 2 mil Pt leads with EPOTEK silver epoxy. Excitation currents used were typically 10 mA with a measurement frequency of 31 Hz.

III. RESULTS AND DISCUSSION

A. Temperature dependent resistivity

Resistivity versus temperature curves for $Co_2MnSi_{1-x}Al_x$ measured in zero field and normalized by their values at 2 K are shown in Fig. 2. The most obvious feature is the remarkably high residual resistivity ratio (RRR) of ~4.5 for Co_2MnSi, in sharp contrast to the others in the series which display a relatively small, systematically decreasing RRR with increasing Al content. In fact, the measured residual resistivity of ~3 $\mu\Omega$ cm for the polycrystalline Co_2MnSi compares well with reported values for single crystal boules (~2.5 $\mu\Omega$ cm)[17,18] and epitaxial films (~15 $\mu\Omega$ cm).[19,20] A high RRR value and $\mu\Omega$ cm-range resistivity signify a low level of temperature independent scattering due to sources such as dislocations, impurities, or grain boundaries. Doping naturally introduces disorder; however, it is not believed that this has induced a significant phase separation into the A2 phase. If this were the case, we would not expect to see such a close agreement with the Slater-Pauling rule or Vegard's law. Even so, Heuslers containing Al are known to possess a higher degree of anti-site disorder due to an exchange of atoms on the Mn-Al sites (B2 structure)[6,21] and, since all of our samples were annealed at the same temperature (600 °C), the trend in RRR may be a reflection of the monotonically decreasing order-disorder ($L2_1$-B2) phase transition temperature with increasing Al content (~670 – 1300 °C).[3] Hence, it is likely that some B2-disorder is present in our samples, and that this disorder increases systematically for each sample as $x \to 1$ ($\Delta x = 0.25$).

A minimum in the resistivity is found at 25, 30, 30, 40, and 50 K for samples with $x = 0$, 0.25, 0.5, 0.75, and 1, respectively, and for samples with $x \geq 0.5$ it is followed by an upturn at low temperature. This is a common feature reported for many Heusler alloys and is typically attributed to disorder enhanced coherent backscattering of conduction electrons, a mechanism known as weak localization.[22] Indeed, below the resistivity minimum we find excellent agreement with the $-T^{1/2}$ power law predicted for 3D disordered metals (see Fig. 3). Nonetheless, the weak localization theory predicts that these upturns may be suppressed by the application of a magnetic field, a behavior which could not be verified due to the interference of a large anomalous Hall effect contribution, to be discussed later.

Above the resistivity minima, we observed conduction behavior ranging from metallic ($x = 0$) to semiconducting ($x = 1$). For the $x = 0$ and 0.25 samples, a linear T-dependence is followed from ~100 K to room temperature indicating that the resistivity is dominated by electron-phonon scattering in this range. Between about 50 K and 100 K, the $x > 0$ samples can be best fitted to a $\sim T^2$ temperature dependence as seen in Figs. 3(a)–3(e). Two theories which predict a quadratic temperature dependence are Fermi-liquid theory (electron-electron scattering) and single-magnon scattering (a spin-flip process). The latter is usually deemed forbidden in half-metal ferromagnets due to the lack of minority-spin charge carriers (a notable exception is an *anomalous* single-magnon mechanism, which predicts a T^3 dependence, recently observed in the half-metallic ferromagnet $R_{0.6}Sr_{0.4}MnO_3$; R = Sm and $Nd_{0.8}Tb_{0.2}$)[23] and is replaced by a double-magnon scattering

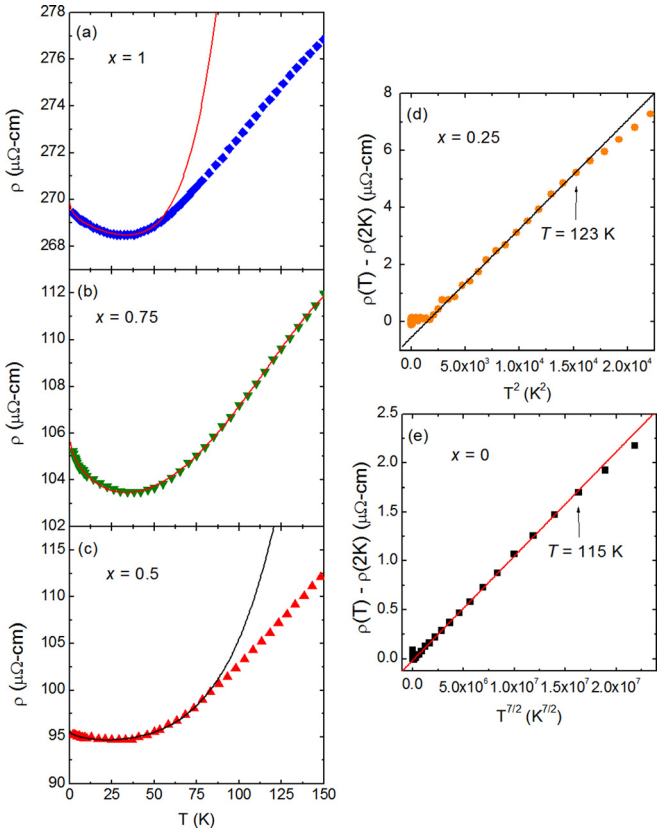

FIG. 3. Fitted curves of the low temperature resistivity of $Co_2MnSi_{1-x}Al_x$. (a)–(c) The solid lines are fits to the equation $\rho(T) = \rho_0 - aT^{1/2} + bT^2 + cT^5$. (d) and (e) The solid lines are fits to the equation $\rho(T) - \rho_0 = aT$.

process with a $\sim T^{9/2}$ dependence at low temperature and $\sim T^{7/2}$ at higher temperatures.[24,25] However, band structure calculations of $Co_2MnSi_{1-x}Al_x$ do predict that a small fraction of minority-spin carriers exist at the Fermi level for $x > 0$, which may facilitate the single-magnon process. In contrast, Fig. 3(e) shows a linear least-squares fit of $\rho(T) - \rho(2K)$ versus $T^{7/2}$ for Co_2MnSi, where we can see that this temperature dependence is followed quite well, from just above the resistivity minimum up to ~115 K.

B. Magnetoresistance and the Hall effect

The Hall resistivity curves as a function of magnetic field for $Co_2MnSi_{1-x}Al_x$ at 2 K for $x \neq 0$ are shown in Fig. 4. The data are comprised of two distinct field regions separated by a knee representing the perpendicular saturation field of the magnetization. The linear, low-field region ($B = 0$ to ~1 T) of the Hall resistivity is due to the AHE, while the high field region, with a much smaller, negative slope, is due to the ordinary Hall effect.[26] Empirically, the total Hall resistivity can be expressed as

$$\rho_H = R_0 B + R_s \mu_0 M, \quad (1)$$

where R_0 is the ordinary Hall coefficient, R_s is the anomalous Hall coefficient, M is the magnetization, and μ_0 is the vacuum permeability. The slope and y-intercept of the linear fit of ρ_H/B vs. $\mu_0 M/B$ are R_s and R_0, respectively.

For consistency, the Hall effect and magnetization experiments were performed on the same samples, and under

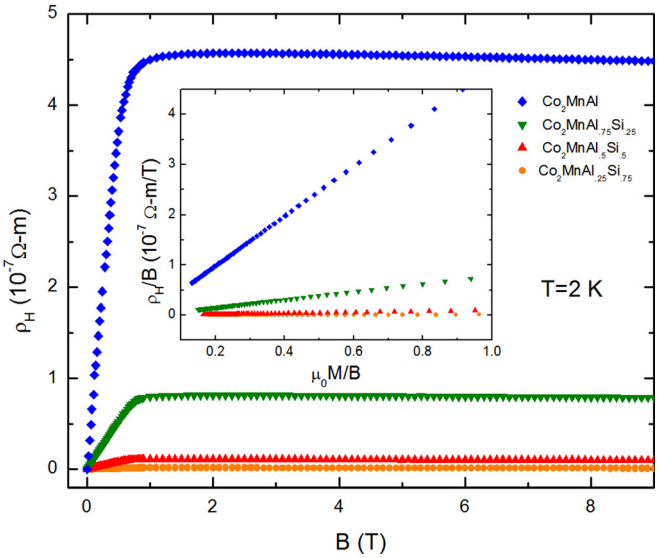

FIG. 4. The Hall resistivity (ρ_H) as a function of magnetic field (B) and concentration (x) at $T = 2$ K. Inset: The linear relationship between ρ_H/B and $\mu_0 M/B$, used to extract the ordinary and anomalous Hall coefficients.

identical temperatures and field orientations. The average of the positive and negative field ρ_H data was used to remove any longitudinal component of the resistivity. Both sets of data were then used in conjunction with Eq. (1) to extract the Hall coefficients (see inset of Fig. 4). In this way, we were able to avoid an overestimation of these parameters since the magnetization does not saturate at high field (~7 T). The temperature dependent charge carrier densities (n) and carrier type (electrons or holes) can then be determined by $R_0 = \pm 1/n(T)e$. Figs. 5(a) and 5(b) show $n(T)$ and $R_s(T)$ in the upper and lower panels, respectively. The series shows electron-like conduction with very little temperature dependence and a trend of increasing n with increasing Si content. Although we could not obtain the carrier concentration for Co_2MnSi, we expect that it takes the highest value of the

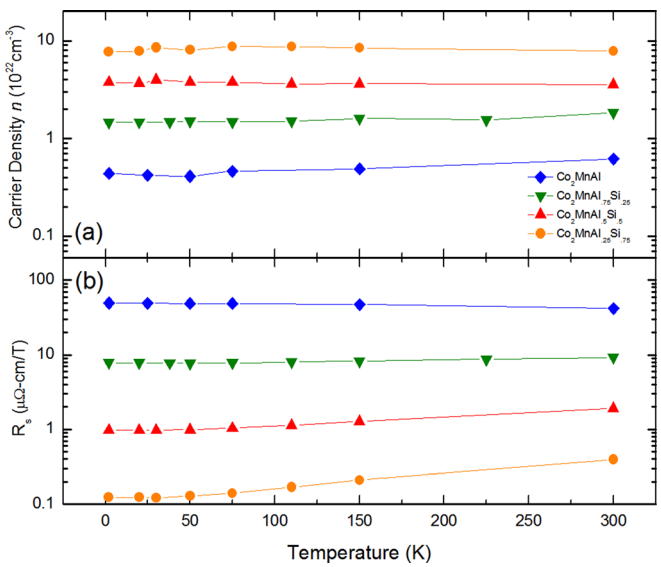

FIG. 5. (a) The charge carrier density (n) as a function of temperature derived from R_0 for $Co_2MnSi_{1-x}Al_x$ shown on a semi-log scale. (b) The anomalous Hall coefficient as a function of temperature shown on a semi-log plot.

series, based on the correlation between the ρ_0 values and n. We also note that the formula used above is derived from a single-band model, which cannot treat the situation where electrons and holes coexist.

The upper-right inset of Fig. 6 shows $R_s(T)/R_s(300\,K)$ versus T in order to highlight the differences between the temperature-dependent behaviors throughout the series. The temperature dependence of R_s originates from the T-dependence of the longitudinal resistivity, and they are related to each other by

$$R_s \sim \rho_{xx}^{\beta}, \tag{2}$$

where $\rho_{xx} = \rho_{xx0} + \rho_{xxT}$, and ρ_{xx0} and ρ_{xxT} are the residual and temperature-dependent resistivities, respectively. The value of the exponent can be used to elucidate the dominant scattering mechanism in the material: $\beta = 1$ corresponds to asymmetric spin-orbit scattering (skew-scattering), and $\beta = 2$ corresponds to side-jump processes and intrinsic band structure effects. β has been observed to take non-integer values, depending on the quality of the metal and degree of conductivity. Since one or more of these mechanisms may contribute to the total AHE, their relative contributions are typically found by fitting to the relation,

$$R_s \sim a\rho_{xx} + b\rho_{xx}^2, \tag{3}$$

where a and b are weighting coefficients associated with the scattering of $\beta = 1$ and 2, respectively. If the skew-scattering term $a\rho_{xx}$ is then replaced by $a'\rho_{xx0} + a''\rho_{xxT}$, Eq. (3) can be used to distinguish defect (i.e., residual) from temperature-dependent scattering.[27] In Heusler alloys, this detailed analysis may be necessary due to the fact that their spin-polarized band structures are highly sensitive to anti-site disorder, linking their RRR values directly to any intrinsic contributions to R_s, as well.

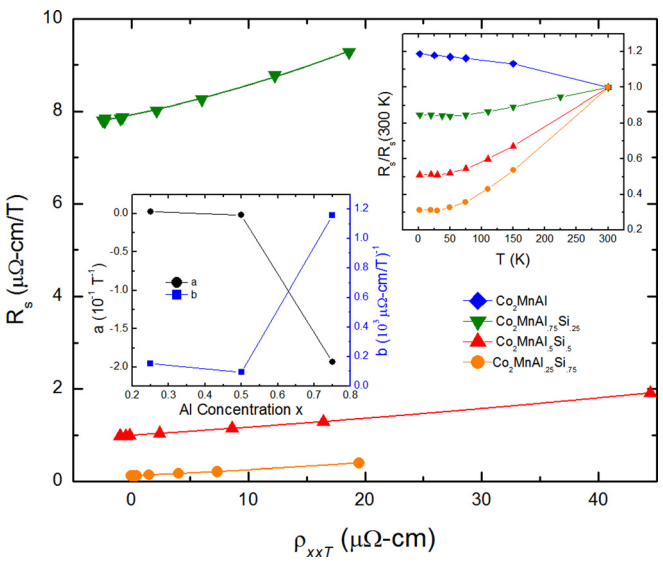

FIG. 6. The anomalous Hall coefficient (R_s) as a function of the temperature dependent component of the resistivity (ρ_{xxT}). The solid lines are fits to Eq. (4). Right inset: The R_s normalized by their values at 300 K. Left inset: The skew-scattering parameter (a) and the intrinsic-scattering parameter (b) as a function of Al concentration (x).

Studies of this type involve systematically varying ρ_{xx0} in a set of samples with the same nominal composition, which is beyond the scope of this paper. However, we can interpret our data based on an analysis by Vidal *et al.*,[28] which addresses some of these concerns. After substituting the full expression for ρ_{xx} into Eq. (3) and rearranging terms, we can express the anomalous Hall coefficient as a sum of temperature-dependent and -independent parts,

$$R_s \sim \rho_{AHE,0} + (a + 2b\rho_{xx0})\rho_{xxT} + b\rho_{xxT}^2, \tag{4}$$

where $\rho_{AHE,0} = a\rho_{xx0} + b\rho_{xx0}^2$ is the residual anomalous Hall resistivity. By plotting ρ_{xxT} versus R_s, the data can be fitted to a quadratic equation. Using the values of ρ_{xx0} obtained earlier, the scattering parameters a and b can now be extracted.

Although it is still a matter of debate how disorder and weak-localization affect the scaling of the AHE, Fig. 6 shows that the data are still well fit by Eq. (4) throughout the measured temperature range. Recall that the $x = 0.5$, 0.75, and 1 samples all exhibit a $-T^{1/2}$ temperature dependence of their resistivity below ~50K. In the case of $x = 0.5$ and 0.75, this region accounts for ~1.3% and ~10% of the overall change in resistivity between 2 and 300 K, respectively. However, in the case of $x = 1$ (Co_2MnAl) where this region accounts for ~7.5% of the resistivity change, the value of ρ_{xx0} is also well above the so-called "Mooij criterion," $\rho_{xx0} \cong 150\,\mu\Omega$ cm, a qualitative threshold above which e-e interactions reverse the sign of the temperature coefficient of resistance from positive to negative, and weak-localization effects extend to higher temperatures.[22] A sign of the failure of the scaling relation for this sample ($x = 1$) is the drastically different temperature dependences of ρ_{xx} and R_s.

In Fig. 5(b), we saw that the overall R_s values decreased by nearly an order of magnitude as the Al concentration decreased. In order to determine if this trend originates from changes in the relative contributions of the various scattering mechanisms across the series, we plot the scattering parameters a and b versus Al concentration for the $x = 0.25$, 0.5, and 0.75 samples in the lower-left inset of Fig. 6. Now the reason for the smaller magnitudes of R_s for the $x = 0.25$ and 0.5 samples is clear: both their skew-scattering parameters and their intrinsic-scattering parameters are very small, on the order of 10^{-3} T^{-1} and 10^{-4} $(\mu\Omega\ \text{cm})^{-1}$, respectively. These values are similar to those obtained for the Heusler alloys $Co_2Fe(Si, Al)$.[29] However, as the Al concentration increases to 0.75, a crossover occurs where both the intrinsic and skew-scattering contributions to the AHE rise dramatically to $\sim 10^{-3}$ $(\mu\Omega\ \text{cm})^{-1}$ and $\sim 10^{-1}$ T^{-1}, respectively. This is also reflected in the increased curvature of the ΔR_s versus $\Delta\rho_{xxT}$ plot of the $x = 0.75$ data. The trend is consistent with recent theoretical predictions that the intrinsic Berry phase contribution should be very large in Co_2MnAl but rather small in Co_2MnSi.[12] This may also be why we were unable to detect an AHE signal in Co_2MnSi but were able to observe extremely large magnitudes in Co_2MnAl. According to Eq. (4), if high quality single-crystals of Co_2MnAl that have smaller values of ρ_{xx0} could be made, the linear term

would become much smaller and the intrinsic contribution would dominate. This would be interesting because then a baseline could be acquired for a systematic study of the effects of disorder on a material with a prominent intrinsic AHE.

IV. CONCLUSIONS

We have explored the electrical transport properties of the quaternary Heusler alloys $Co_2MnSi_{1-x}Al_x$ ($x = 0$, 0.25, 0.5, 0.75, and 1), and found trends that are consistent with a transition, which occurs across the series, from a partially spin-polarized compound with a large AHE ($x = 1$), to one with the temperature-dependent resistivity of a half-metallic ferromagnet ($x = 0$). The resistivity exhibits a transition in temperature dependence below $\sim$100 K from a $\sim T^{7/2}$ power law for $x = 0$, to a $\sim T^2$ power law for $x = 0.25$, followed by a $-T^{1/2}$ power law for $x \geq 0.5$, which are due to high-T double-magnon scattering, Fermi-liquid *e-e* interactions (or single-magnon scattering), and coherent back-scattering (i.e., weak-localization), respectively. The residual resistivity at $T = 2$ K increases with increasing Al content, likely reflecting the increase in the $L2_1$/B2 order-disorder transformation temperature which occurs with increasing Si content, resulting in a higher degree of B2 disorder as the Al content is increased. Finally, we have shown that the growth of the AHE with increasing Al content is caused by a systematic increase in both the extrinsic and intrinsic scattering mechanisms.

ACKNOWLEDGMENTS

S. Stadler acknowledges support from the National Science Foundation Grant No. NSF-DMR-0965009. P. W. Adams acknowledges support from the US DOE, BES, MSE Grant No. DE-FG02-07ER46420. D. P. Young acknowledges support from the National Science Foundation Grant No. NSF-DMR-1306392.

[1]K. Ozdogan, E. Sasioglu, and I. Galanakis, J. Appl. Phys. **103**(2), 023503–023510 (2008).
[2]Y. Sakuraba, K. Takanashi, Y. Kota, T. Kubota, M. Oogane, A. Sakuma, and Y. Ando, Phys. Rev. B **81**(14), 144422 (2010).
[3]R. Y. Umetsu, K. Kobayashi, A. Fujita, R. Kainuma, and K. Ishida, Scr. Mater. **58**(9), 723–726 (2008).
[4]P. J. Webster, J. Phys. Chem. Solids **32**(6), 1221–1231 (1971).
[5]Y. Sakuraba, M. Hattori, M. Oogane, Y. Ando, H. Kato, A. Sakuma, T. Miyazaki, and H. Kubota, Appl. Phys. Lett. **88**(19), 192508 (2006).
[6]R. Y. Umetsu, K. Kobayashi, A. Fujita, R. Kainuma, and K. Ishida, J. Appl. Phys. **103**(7), 07D718 (2008).
[7]Y. J. Chen, D. Basiaga, J. R. O'Brien, and D. Heiman, Appl. Phys. Lett. **84**(21), 4301–4303 (2004).
[8]E. V. Vidal, G. Stryganyuk, H. Schneider, C. Felser, and G. Jakob, Appl. Phys. Lett. **99**(13), 132509 (2011).
[9]T. Kubota, J. Hamrle, Y. Sakuraba, O. Gaier, M. Oogane, A. Sakuma, B. Hillebrands, K. Takanashi, and Y. Ando, J. Appl. Phys. **106**(11), 113907 (2009).
[10]J. Xingtao, Y. Wei, Q. Minghui, and W. Lei, J. Phys. D: Appl. Phys. **41**(8), 085004 (2008).
[11]I. Galanakis, P. H. Dederichs, and N. Papanikolaou, Phys. Rev. B **66**(17), 174429 (2002).
[12]J. Kübler and C. Felser, Phys. Rev. B **85**(1), 012405 (2012).
[13]H. Schneider, E. Vilanova Vidal, S. Chadov, G. H. Fecher, C. Felser, and G. Jakob, J. Magn. Magn. Mater. **322**(6), 579–584 (2010).
[14]T. Jen-Chuan and G. Guang-Yu, New J. Phys. **15**(3), 033014 (2013).
[15]L. Ritchie, G. Xiao, Y. Ji, T. Y. Chen, C. L. Chien, M. Zhang, J. Chen, Z. Liu, G. Wu, and X. X. Zhang, Phys. Rev. B **68**(10), 104430 (2003).
[16]A. R. Denton and N. W. Ashcroft, Phys. Rev. A **43**(6), 3161–3164 (1991).
[17]M. P. Raphael, B. Ravel, M. A. Willard, S. F. Cheng, B. N. Das, R. M. Stroud, K. M. Bussmann, J. H. Claassen, and V. G. Harris, Appl. Phys. Lett. **79**(26), 4396–4398 (2001).
[18]M. P. Raphael, B. Ravel, Q. Huang, M. A. Willard, S. F. Cheng, B. N. Das, R. M. Stroud, K. M. Bussmann, J. H. Claassen, and V. G. Harris, Phys. Rev. B **66**(10), 104429 (2002).
[19]W. H. Wang, X. B. Ren, G. H. Wu, M. Przybylski, J. Barthel, and J. Kirschner, IEEE Trans. Magn. **41**(10), 2805–2807 (2005).
[20]L. J. Singh, Z. H. Barber, Y. Miyoshi, Y. Bugoslavsky, W. R. Branford, and L. F. Cohen, Appl. Phys. Lett. **84**(13), 2367–2369 (2004).
[21]K. Özdoğan, E. Şaşıoğlu, B. Aktaş, and I. Galanakis, Phys. Rev. B **74**(17), 172412 (2006).
[22]P. A. Lee and T. V. Ramakrishnan, Rev. Mod. Phys. **57**(2), 287–337 (1985).
[23]T. Akimoto, Y. Moritomo, A. Nakamura, and N. Furukawa, Phys. Rev. Lett. **85**(18), 3914–3917 (2000).
[24]M. I. Katsnelson, V. Y. Irkhin, L. Chioncel, A. I. Lichtenstein, and R. A. de Groot, Rev. Mod. Phys. **80**(2), 315–378 (2008).
[25]V. Y. Irkhin and M. I. Katsnelson, Eur. Phys. J. B **30**(4), 481–486 (2002).
[26]N. Nagaosa, J. Sinova, S. Onoda, A. H. MacDonald, and N. P. Ong, Rev. Mod. Phys. **82**(2), 1539–1592 (2010).
[27]Y. Tian, L. Ye, and X. Jin, Phys. Rev. Lett. **103**(8), 087206 (2009).
[28]E. Vilanova Vidal, H. Schneider, and G. Jakob, Phys. Rev. B **83**(17), 174410 (2011).
[29]I. M. Imort, P. Thomas, G. Reiss, and A. Thomas, J. Appl. Phys. **111**(7), 07D313 (2012).